https://doi.org/10.3311/PPch.41256

Periodica Polytechnica Chemical Engineering, 69(3), pp. 417–426, 2025

Enhancing Carbon Dioxide Separation Efficiency in Mixed Matrix Membranes Using Titania Nanoparticles and Polyether Sulfone

Tayyib Murtaza[1], Muhammad Zia-ul-Haq[1], Naveed Ramzan[1], Muhammad Mubashir[2], Asif Jamil[1,3*]

[1] Chemical, Polymer and Composite Materials Engineering Department, University of Engineering and Technology Lahore, 39021 Lahore, Pakistan
[2] Water Technologies Innovation Institute & Research Advancement, Saudi Water Authority (WTIIRA-SWA), 35417 Jubail, Saudi Arabia
[3] Department of Mechanical Engineering, Kaunas University of Technology, K. Donelaičio St. 73., 44249 Kaunas, Lithuania
* Corresponding author, e-mail: majamil@uet.edu.pk

Received: 12 June 2025, Accepted: 25 August 2025, Published online: 16 September 2025

Abstract

Membrane science is an advanced, environmentally sustainable technology that provides distinct advantages over traditional methods for CO_2 capture and separation. In this study, mixed matrix membranes were synthesized by incorporating varying concentrations of titania into polyethersulfone using the phase-inversion technique for the separation of CO_2/CH_4 and CO_2/N_2 gas mixtures. Thermal, chemical and morphological analysis demonstrated the beneficial impact of TiO_2 on the performance of MMMs, particularly when compared to the pristine membrane. Moreover, the TiO_2 loading was shown to improve gas separation performance by reducing the thickness of the dense layer and increasing permeability through uniform filler dispersion. The highest value of optimum selectivity (CO_2/CH_4) was attained with 3 wt% TiO_2 loading, which is 22.3% more than that of the pristine membrane. This performance is attributed to strong interfacial interactions between polyethersulfone and TiO_2 at this specific loading, as illustrated by the morphological diagram.

Keywords

mixed matrix membrane (MMM), polyethersulfone (PES), titania nanoparticles, CO_2 separation, polymer membrane

1 Introduction

The escalating levels of carbon dioxide emissions due to anthropogenic activities have emerged as a critical global challenge, necessitating innovative approaches for effective greenhouse gas mitigation [1]. Between 1990 and 2013, the burning of fossil fuels and industrial flue gases was the main source of the 61% increase in CO_2 emissions in the atmosphere [2]. In particular, the separation of CO_2 from methane is essential for enhancing the sustainability of natural gas utilization and reducing the carbon footprint. Among the various methodologies employed for this separation, the convergence of economic viability, manufacturing simplicity, and outstanding selectivity prospects has propelled polymeric membranes to prominence [3].

Membranes are typically made of either inorganic or polymeric materials and combining both types has proven advantageous in terms of reducing manufacturing costs, enhancing chemical and thermal stability [4–6]. The development of mixed matrix membranes (MMMs), which incorporate both inorganic and polymeric materials, is challenging, particularly in achieving a flawless or minimally affected morphology. The success of MMMs depends on selection of appropriate materials, as poor material choice can result in interfacial defects that significantly compromise the membrane separation efficiency. Therefore, the compatibility of the polymer-filler systems is crucial for successful membrane formation.

The efficiency of polymeric membranes in gas separation is influenced by their structural and chemical properties, which affect both gas solubility and diffusion rates [7]. The method of membrane fabrication plays a crucial role in determining polymer chain arrangement and the distribution of free volume, both of which are critical to gas transport behavior. A higher and well-connected free volume enhances permeability without severely

Cite this article as: Murtaza, T., Zia-ul-Haq, M., Ramzan, N., Mubashir, M., Jamil, A. "Enhancing Carbon Dioxide Separation Efficiency in Mixed Matrix Membranes Using Titania Nanoparticles and Polyether Sulfone", Periodica Polytechnica Chemical Engineering, 69(3), pp. 417–426, 2025. https://doi.org/10.3311/PPch.41256

compromising selectivity, allowing the membrane performance to approach the Robeson upper bound [8]. Additionally, introducing CO_2 affinity due to groups such as ether and carbonyl functional groups increases the membrane affinity for CO_2 through dipole–quadrupole interactions, leading to improved solubility [9].

Polyethersulfone (PES) is widely favored among commercial polymers for membrane fabrication due to its rigid aromatic structure, excellent thermal and chemical resistance, and strong resistance to plasticization and physical aging [9]. The presence of ether and sulfone linkages contributes to both structural robustness and moderate CO_2 solubility, offering a reliable balance of performance [10]. Compared to cellulose acetate (CA), PES shows better durability in humid and chemically aggressive environments, and unlike polyimides which may suffer from CO_2-induced plasticization, PES maintains structural integrity over prolonged operation. These combined properties make PES a dependable material for developing high-performance gas separation membranes [11]. Solvent selection also plays a critical role in determining membrane morphology, porosity, and overall performance, as each solvent interacts differently with the polymer and non-solvent during phase inversion [12]. Solvents such as N,N-dimethylformamide (DMF) and N,N-dimethylacetamide (DMAc), although effective in dissolving PES, evaporate more quickly and are more toxic, often resulting in surface defects and inconsistent pore formation. Dimethyl sulfoxide (DMSO) tends to cause pore collapse due to its high hydrophilicity, while low-polarity solvents like tetrahydrofuran (THF) and acetone are incapable of dissolving PES effectively, making them unsuitable for membrane fabrication [12]. N-methyl-2-pyrrolidone (NMP) is widely used with PES due to its excellent miscibility, high boiling point, and a solubility parameter closely matching that of PES, which ensure uniform polymer dissolution and controlled phase inversion. Its slower evaporation rate promotes gradual demixing during membrane formation, facilitating well-developed pore structures and reduced macrovoids [13].

A membrane permeability and selectivity are commonly used to evaluate its performance. CA is often used as a reference material in gas processing, exhibiting a selectivity range of 10 to 15 [14]. Research indicates that polymeric materials generally show a trade-off between permeation and selectivity (Robeson plot) [3]. This indicates that enhancing permeability often results in a decrease in selectivity and *vice versa*. To address these performance limitations, MMMs have emerged, which incorporate inorganic materials within a polymeric matrix. Metal oxides nanoparticle, and others are examples of inorganic fillers that have been used and discussed in the literature [3, 15]. However, a number of parameters significantly impact the gas transport behavior of polymer/inorganic MMMs including the characteristics of polymers and inorganic nanoparticles, their miscibility and interfacial defects, structure [16].

Minimizing the thickness of the dense layer is essential for achieving high gas flux. As a result, anisotropic membranes with a dense skin layer on top are often preferred, as they can offer both high flux and gas selectivity. Several factors interact during the membrane fabrication process, including air-drying time, polymer concentration, ambient humidity, coagulant bath activity, and others [17, 18]. Together, these elements affect the membrane shape and performance [19].

The creation of voids at the particle-polymer interface is a major issue in the production of MMMs. One of the key factors for successful MMMs production is ensuring the proper dispersion of nanoparticles within the polymer matrix. Previous studies have shown that nanoparticles with small sizes and high surface areas tend to disperse more effectively in polymer matrices [20]. Commonly used nanoparticles in MMMs include fumed silica, TiO_2, and MgO [11, 15, 21, 22]. However, research has demonstrated that fumed silica, when used in MMMs, tends to chemically bond with itself, making it difficult to disperse either separately or in nanoscale [21, 23]. On the contrary, MgO have limitations, like their tendency to react with water and the polymer matrix, as well as their propensity to form microscale aggregates, which hinders their use in MMMs [24, 25].

TiO_2 nanoparticles are widely recognized for their ability to improve membrane hydrophilicity and resistance to fouling. However, their practical application is often limited by challenges such as particle agglomeration, inadequate dispersion at higher concentrations, and the potential for nanoparticle leaching. In addition, the integration of TiO_2 with PES membranes, particularly through surface modification or chemical functionalization, remains insufficiently studied. Addressing these limitations requires further research into the development of environmentally benign solvent systems, structurally stable nanocomposites, and cost-effective, scalable surface engineering methods to optimize the performance of PES/TiO_2 membranes in separation processes.

Most previous studies involving TiO_2-based MMMs have focused on dense or flat-sheet composite membranes,

often using polymers such as polyimide or polysulfone (PSF) prepared *via* solution casting or dip-coating methods. While these approaches provide a good degree of filler dispersion and mechanical integrity, but they are limited in terms of scalability and typically result in high transport resistance due to membrane thickness. The present study develops asymmetric PES–TiO_2 MMMs using the non-solvent induced phase separation (NIPS) technique, also known as dry/wet phase inversion, which is widely used in industry for scalable membrane production. This method allows for the fabrication of membranes with a thin selective skin layer and porous substructure, reducing gas transport resistance while maintaining mechanical support. Moreover, PES has been relatively underutilized in gas separation MMMs despite its excellent film-forming properties, thermal stability, and resistance to plasticization.

This study looked at how TiO_2 nanoparticles affected the gas transport characteristics of MMMs based on polyether sulfone. With a higher specific surface area (500 $m^2 \cdot g^{-1}$) and a particle size (21 nm), TiO_2 offer improved dispersion and avoid the formation of undesired voids at the nanoparticle–polymer interface. Unlike some other nanoparticles, TiO_2 does not naturally fuse together, allowing it to disperse effectively as individual particles or in nanoscale aggregates. Based on these characteristics, TiO_2 was selected for this study. The studies suggest that TiO_2 not only improves CO_2/CH_4 separation performance but also aligns with established trade-off trends observed in gas separation literature [11, 26, 27].

2 Materials

PES (ULTRASON® E-6020 P), with a molecular mass of approximately 50,000 $g \cdot mol^{-1}$, was obtained from BASF (Germany). The solvent used was NMP (C_5H_9NO, b.p. 475.15 K, > 99.9% purity) and was acquired from Merck KGaA dealers in Lahore, Pakistan. TiO_2 nanoparticles (average particle size ~21 nm, surface area ~50 $m^2 \cdot g^{-1}$, purity ≥99%) were purchased from Sigma Aldrich USA. The physical and chemical properties of the materials are shown in Table 1.

2.1 Preparation of MMM dope solution

PES flakes and TiO_2 nanoparticles were dried at 333.15 K for 24 h to remove adsorbed water. MMMs were created by adding TiO_2 particles (1, 3, and 5 wt%) to the NMP and stirring for 24 h. The mixture was ultrasonicated to ensure excellent TiO_2 particle dispersion in the NMP. PES (20 wt%) was added in two steps: the first step involved adding 10 wt% of the total PES to the TiO_2 and stirring for 60 min. PES then was progressively added over the course of 24 h while gently stirring continuously. The homogenized solution was then degassed.

2.2 Fabrication of asymmetric flat sheet membrane

The membranes were casted at a glass plate by adjusting the film thickness of 200 µm *via* casting blade. Later, the freshly developed membranes were dried for 30 s in the atmosphere before immersing them in a water bath for 24 h. Afterwards, the drying of the immersed membranes was carried out at ambient conditions for a day.

2.3 Permeation test

Permeation behavior of MMMs was evaluated at ambient temperature and 3 bar pressures using N_2, CO_2, and CH_4 gases. After evacuating the system with a vacuum pump, gas flow rates were measured using a soap bubble

Table 1 Physical and chemical properties of materials

Property	PES	NMP	TiO_2
Chemical nature	Aromatic thermoplastic polymer with ether and sulfone groups	Polar aprotic organic solvent with a lactam ring	Inorganic compound with amphoteric behavior
Appearance	Amber or transparent solid	Colorless to pale yellow liquid	White crystalline powder
Boiling point (K)	Not applicable (thermoplastic)	475.15 K	Not applicable
Melting point (K)	~230 (glass transition)	249.15 K	Not applicable
Solubility	Insoluble in water; soluble in NMP, DMF, DMAc	Miscible with water and organic solvents	Insoluble in water and organic solvents
Thermal stability	High (~503.15 K glass transition)	Moderate	Very high
Key attributes	High mechanical strength, thermal stability, good film formation	Excellent solvent for PES, slow evaporation, good pore control	Photocatalytic (anatase), UV resistance, enhances membrane properties

flowmeter, recording the time for the bubble to move between reference points. Permeability (P) and selectivity calculations for the permeated gases were based on Eqs. (1) and (2) respectively [10]:

$$\frac{P_i}{l} = \frac{Q_i}{T_i} \times \frac{273}{A\Delta p_i}, \tag{1}$$

$$\alpha = \frac{P_{CO_2}/l}{P_{CH_4}/l}, \tag{2}$$

where Q is the volumetric flow rate ($cm^3 \cdot s^{-1}$), T is the temperature (K), A is the effective area of the membrane (cm^2), Δp_i is the trans-membrane pressure (Pa), l is the membrane thickness (cm), α is the selectivity, and i is for incident gas (it could be CO_2 or CH_4 in this case).

2.4 Membrane characterization

Scanning electron microscopy (SEM) (Nova NanoSEM 450, Thermo Fisher Scientific, Hillsboro, USA) analysis was used to examine the morphology of the cast membranes. Fourier-transform infrared spectroscopy (FTIR) (Perkin Elmer 1650, PerkinElmer, Waltham, USA) identifies the functional groups that were affixed to the produced membranes. Under the transmission mode, the spectra of every membrane were acquired within the 400–4000 cm^{-1} range. To ascertain the thermal stability of PES MMMs, thermogravimetric analysis (TGA, STA6000, PerkinElmer, Waltham, USA) was utilized. The heating rate was 283.15 K min^{-1} throughout a temperature range of 303.15 to 1073.15 K, the thermal behavior was examined in nitrogen environment.

3 Results and discussion

3.1 Chemical analysis of the membranes

The FTIR spectra of the membranes that were made are shown in Fig. 1. The intrinsic ether (−C−O−C−) linkage, aromatic benzene groups (C_6H_6) peaks, and sulfone (O=S=O) bands linked to PES were seen for all membranes. Spectral characteristics of the band positions and assignments that were discovered are in good agreement with previous research [26–28]. Furthermore, the adsorbed water caused OH stretching vibrations. Because of the Ti−O interaction and the little change in peak position caused by hydrogen bonding, the effect of embedding TiO_2 particles was seen in the enhanced intensity of peaks in the 450–800 cm^{-1} range [28]. Peaks related to C−O−C stretching vibration are located between 1100 and 1250 cm^{-1}. Peaks that correspond to C−H bending vibration are located between 1300 and 1400 cm^{-1} [26, 27]. Peaks around 1100–1250 cm^{-1} are associated with C−O−C

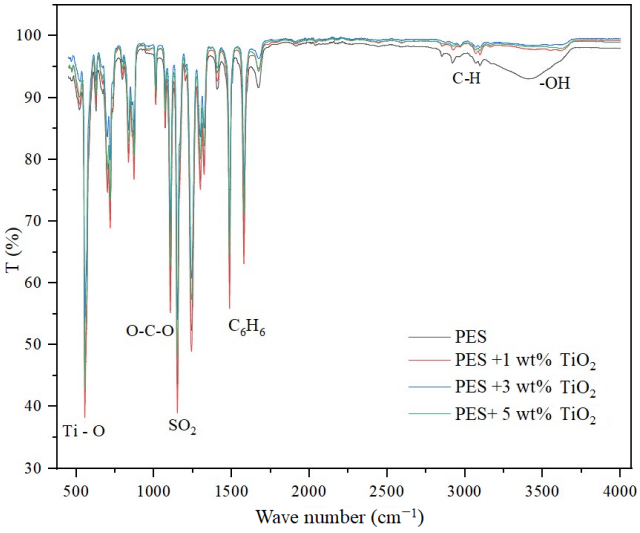

Fig. 1 FTIR analysis of PES, and MMMs at various titania nanoparticle loadings

stretching vibration. Peaks around 1300–1400 cm^{-1} correspond to C−H bending vibration. Peaks around 1600–1700 cm^{-1} are associated with C=O stretching vibrations in carbonyl groups. Finally, peaks around 2800–3000 cm^{-1} correspond to C−H stretching vibration.

Results suggests a strong linkages between the TiO_2 particles and the PES matrix, leading to a modified membrane structure. The physical interaction between the tiatania and polyether sulfone was demonstrated by the FTIR of the produced membranes.

3.2 Thermal analysis of the developed membranes

TGA shows that the incorporation of inorganic fillers into PES membranes significantly enhanced their thermal stability. TGA curves for MMMs shifted towards higher temperatures, indicating improved thermal resistance. The neat PES membrane and MMM thermograms are shown in Fig. 2. For all membranes, two primary mass loss phases were noted. The agglomerated polymer opening was credited with the first step, which occurred at 473–573 K. There is no mass loss below this temperature, indicating that the membrane matrix is free of moisture and solvent residue. The signal around 773.15 K was linked to the molecular breakage of the polymer chain because of overheating during the subsequent mass loss stage. However, as compared to a pure PES membrane, all MMMs showed a higher degradation temperature. Furthermore, when more heat was absorbed by the TiO_2 particles, the degradation temperature rose in parallel with the rise in TiO_2 loading. Thus, the addition of TiO_2 particles resulted in increased thermal stability [28, 29].

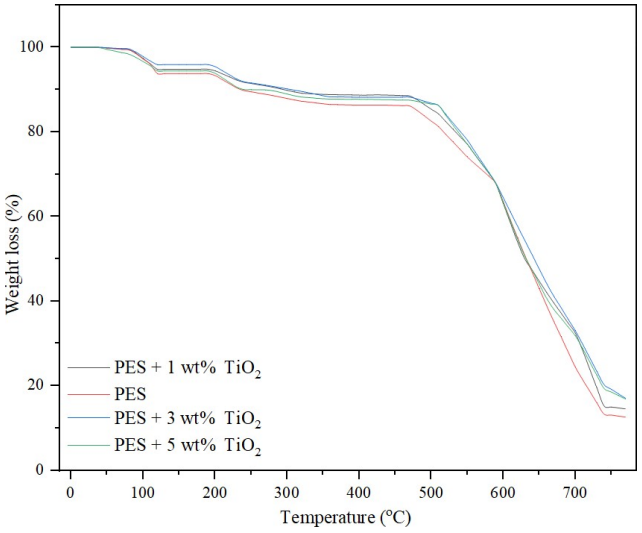

Fig. 2 TGA analysis of developed membranes

3.3 Morphology analysis

Properties of gas movement are highly dependent on the resulting membrane morphology. The structure and shape of the pure PES membrane and MMMs, as well as the titania particle interfacial interactions, were examined using SEM. Fig. 3 shows the cryo-fractured membrane cross section. TiO_2 nanoparticles, a hydrophilic additive with nonsolvent qualities, were used in this study. Their presence increased the thermodynamic instability of the cast film, which in turn caused instantaneous demixing in the coagulation bath and, ultimately, the formation of macro-voids in the membrane structure [20, 28, 30, 31]. Therefore, more macro-voids and porous structures were formed when hydrophilic TiO_2 nanoparticles were added. Fig. 3 illustrates how TiO_2 nanoparticles affect the developed membrane structure. The size of the macro-voids and the thickness of the membrane are particularly noticeable, which illustrates the structural variations brought about by the addition of TiO_2 nanoparticles at 1 to 5 wt%.

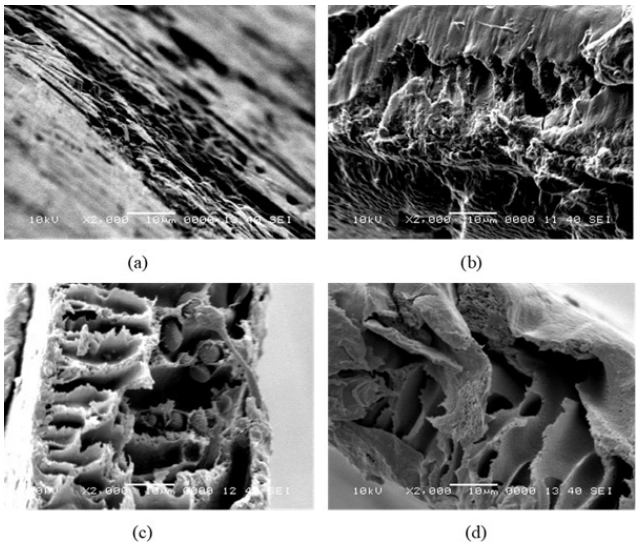

Fig. 3 SEM analysis of: (a) PES; (b) 1 wt% TiO_2; (c) 3 wt% TiO_2; (d) 5 wt% TiO_2 (the scalebars mark 10 µm)

This unique morphological evolution is expected to enhance gas separation performance, as the finger-like voids provide additional pathways for gas molecules to traverse the membrane. The synergistic combination of the high surface area of titania and the inherent selectivity of PES is likely to result in improved separation efficiency, making these membranes promising candidates for various gas separation applications. Membrane was casted with a thickness of around 200 µm.

3.4 PES and titania gas permeation behavior

The CO_2, CH_4, and N_2 permeability of both the pristine and MMMs at varying titania loadings is shown in Fig. 4. The relatively low permeability of the pristine PES membrane is attributed to its rigid glassy polymer structure, which results from the stiff polymer chains [32, 33]. The dualsorption model, in line with Henry's law and Langmuir behavior, explains the mechanisms through which gas molecules interact with and move through the polymer matrix. According to Langmuir behavior, the presence of micro-gaps in glassy polymers facilitates this interaction. Additionally, the permeability of gases through membranes is influenced by both the solubility and diffusivity of the gas molecules. While the diffusivity depends on the molecular size and shape of the gases, solubility is a thermodynamic characteristic linked to the gas condensability at the membrane surface [34].

It is observed that pure PES has lower permeation behavior compared to membranes incorporating titania nanoparticles. PES membranes, with their high glass transition temperature T_g of approximately 493.15 K, remain in a glassy state at room temperature. In glassy polymers like PES, the free volume is relatively low, leading to restricted diffusion rates. This reduced free volume contributes to

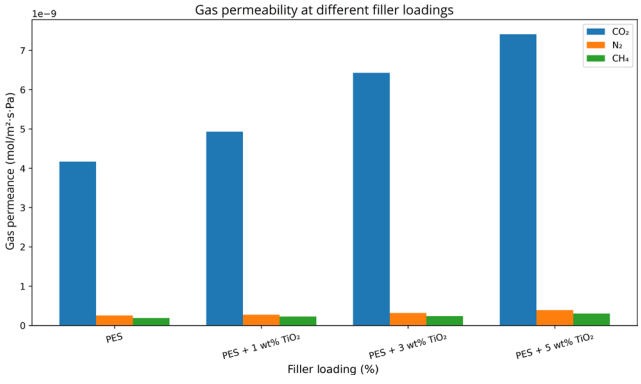

Fig. 4 Gas permeation behavior of developed membranes

a lower diffusion coefficient, impacting the overall gas permeability. Compared to CH_4 and N_2 gases, CO_2 has a greater condensability and solubility towards the glassy PES membrane because of its polar character. In addition to its solubility, the linear molecular form and smaller kinematic diameter of CO_2 allow quick diffusion across the membranes, $CO_2 > N_2 > CH_4$ [27]. That is why we have seen higher permeation of CO_2 in Fig. 4.

Adnan et al. [26] studied the PES/NMP systems. They study successfully fabricated PES membranes for gas separation with varying concentrations. The results highlight the crucial role of polymer concentration in forming a selective skin layer, enabling efficient gas separation. Notably, increasing PES concentration reduced the finger-like structures across the membrane and increased the membrane thickness. Gas flux peaked at lower concentrations, but with compromised CO_2/N_2 and CO_2/CH_4 selectivity. Conversely, higher concentrations yielded improved selectivity.

Here we have chosen the 20 wt% PES concentration and optimize the titania loading to have a better gas flux. Incorporating TiO_2 nanoparticles into PES can alter the polymer morphology, free volume, and overall structure. TiO_2 nanoparticles can act as fillers, which may disrupt the polymer matrix and increase the free volume, potentially enhancing gas permeability [11, 27].

At 1 wt% TiO_2 inclusion, a reasonable polymer attachment was present on the surface of the nonporous TiO_2 particles, resulting in higher gas permeabilities. When 3–5% TiO_2 was added to the MMMs, the contacts between CO_2 and TiO_2 particles were greater than the CH_4–TiO_2 interactions, according to the gas permeability change in Fig. 4. Moghadam et al. [27] and Galaleldin et al. [29] have shown a similar pattern by using poly(amide-imide)/TiO_2 and PES/TiO_2 MMM, respectively as summarized in Table 2. The creation of voids at the polymer–filler interface, when titania loading rises over 3 mass percent, is responsible for the increase in the penetration rate of these gases. With TiO_2 loading the CO_2 permeability increased, peaking at 22.12 gas permeance ($mol \cdot m \cdot s^{-1} \cdot Pa^{-1} \cdot 10^{-9}$) at 5 wt% TiO_2 loading.

3.5 Effect of titania loading on selectivity

Titania loading alter the PES membrane selectivity due to better dispersion and avoid formation of undesired voids. Fig. 5 shows the ideal selectivity on different titania loadings, an increasing trend is observed from 22.12 pristine membrane to 3 wt% loading, which is 27.05 for CO_2/CH_4. Similarly for CO_2/N_2 we also observed the increasing trend from pure PES membrane to 3 wt% titania loading which is

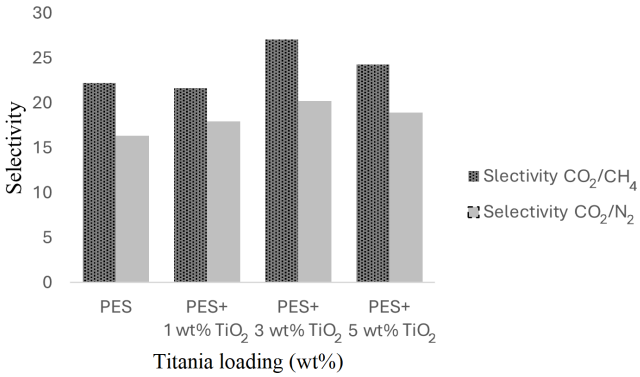

Fig. 5 Gas permeation selectivity of developed membranes

16.3 to 20.22. This shows that the greater dispersion of TiO_2 nanoparticles in the polymer matrix and the advantageous interactions between the hydroxyl groups on TiO_2 and the polar CO_2 molecules are responsible for the improved permeability and selectivity. Therefore it is concluded that PES membranes with titania enhance the CO_2 separation. Liang et al. [11] incorporated inorganic fillers of different shapes (lamellar Na-montmorillonite clays and spherical TiO_2 nanoparticles) in PES membrane and obtained similar results. Liang et al. [11] found the highest selectivty with titania at 4 wt% loading and found a decreasing trend on higher loadings due to interface voids and membrane defects. Also, particle aggregation increased with increasing TiO_2 concentration, and the separation of the more hydrophobic polymer chains from the hydrophilic particle surface produced interface gaps, which led to reduced selectivity and greater gas permeabilities.

Table 2 [11, 27, 29, 35] compares the CO_2 and CH_4 permeability of PES-based membranes with PES–TiO_2 membranes. We see a trade-off between gas permeability and selectivity: as permeability increases selectivity decreases, and *vice versa*. However, in our work we find a balance between permeability and selectivity trade-off on Robeson plot. CO_2 and CH_4 have high permeability in PES–TiO_2 membranes. In particular, at 5 wt% TiO_2 loading, the membrane exhibits enhanced CO_2 and CH_4 permeability along with an improvement in selectivity, approaching the Robeson upper bound.

The performance trends observed in this work align with previous studies: incorporating fillers, especially TiO_2 into a PES matrix increased CO_2 permeability and improved CO_2/CH_4 selectivity, owing to enhanced nanoparticle dispersion and polymer–filler interfacial adhesion. Rashid et al. [36] showed that TiO_2 nanotubes in CA membranes improved CO_2 permeability by over 40% without loss of selectivity, while Maqsood et al. [37] reported that TiO_2 in polyetherimide – polyvinyl acetate (PEI–PVAc) blends

Table 2 Comparison of the fabricated MMMs with the previously developed phase inversion membranes

Dope solution	Fabrication method	TiO_2	CO_2/CH_4 selectivity	Permeation CO_2 ($mol \cdot m^{-2} \cdot s^{-1} \cdot Pa^{-1} \cdot 10^{-9}$)	Pressure (bar)	Ref.
PES/TiO_2, solvent NMP	Dry-wet phase	0 wt%	22.12	4.16	3	This work
		1 wt%	21.64	4.93		
		3 wt%	27.05	6.43		
		5 wt%	24.30	7.40		
PSF/TiO_2, solvent DMF	Wet-wet phase	0 wt%	5.4	2.68	3	[35]
		1 wt%	7.5	1.67		
		3 wt%	36.5	0.67		
		5 wt%	2.1	7.37		
Dope solution	Fabrication method	TiO_2	CO_2/CH_4 selectivity	Permeation CO_2 ($mol \cdot m \cdot s^{-1} \cdot Pa^{-1} \cdot 10^{-15}$)	Pressure (bar)	Ref.
PES/TiO_2, solvent NMP	Dry phase	0 wt%	9.92	1.59	4	[29]
		5 wt%	14.24	2.57		
		10 wt%	4.89	2.84		
		15 wt%	3.7	3.02		
PES/TiO_2, solvent DMF	Dry phase	0 wt%	22.2	0.67	5	[11]
		2 wt%	23	0.77		
		4 wt%	38.5	0.874		
		6 wt%	28.7	0.867		
		10 wt%	18.6	0.961		
		20 wt%	17.3	1.90		
Matrimid/TiO_2, solvent NMP	Dry phase	0 vol%	20.5	1.44	2	[27]
		5 vol%	16.9	1.81		
		10 vol%	14.8	2.48		
		15 vol%	13.8	2.68		
		20 vol%	13.68	3.51		

enhanced the strength, thermal stability, and gas separation performance. These outcomes align with the present work, where PES–TiO_2 membranes achieved high permeability, maintained selectivity, and superior robustness for CO_2 capture and natural gas sweetening.

3.6 Morphological diagram

The permeation properties and behavior of gas molecules through MMMs are governed by the interaction between the polymer matrix and the inorganic nano-filler. Weak interfacial interactions between the polymer chains and the filler surface often led to the formation of interfacial voids, significantly degrading the membrane gas separation performance. Furthermore, the nature of interfacial interactions critically determines the selective transport of one gas over another, directly affecting both gas permeability and selectivity. Poor interfacial compatibility can result in non-ideal morphologies, such as "sieve-in-a-cage", "leaky interface", "plugged interface", and "chain rigidification" [4].

The concept of the "morphological diagram" was introduced by Moore and Koros [38] as a qualitative tool to assess the interactions between nano-sized fillers and the polymer MMMs. Later, Hashemifard et al. [39] compared MMMs from existing literature and evaluated the interfacial interactions between the polymer and inorganic phases, finding the results are in good agreement. Jamil et al. [40] further investigated the interfacial behavior of PEI–clay MMMs, specifically for CO_2 and CH_4 separation performance.

Fig. 6 illustrates the morphological diagram, which is divided into two main sections: ideal morphology and non-ideal morphology. The non-ideal morphologies, which significantly influence gas transport in MMMs, are classified into five distinct cases. **Case I** represents "matrix rigidification", where good adhesion is observed, but the polymer becomes rigidified around the filler, leading to reduced gas permeation while enhancing selectivity. **Case II** depicts the "sieve-in-a-cage" morphology, characterized by higher permeability but nearly unchanged or slightly lower

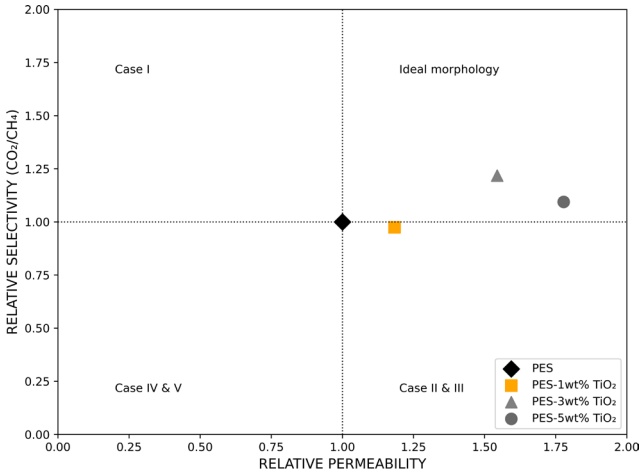

Fig. 6 The PES and TiO_2 MMMs interfacial interactions study *via* the morphological diagram

selectivity. **Case III**, labeled as the "leaky interface", shows a significant increase in gas permeation with only a marginal decrease in selectivity. Finally, **Case IV** and **Case V** describe filler "pore blockage", where permeation decreases at the expense of selectivity [40].

The experimental data for PES-TiO_2 MMMs were analyzed using morphological diagrams to assess interfacial morphologies based on gas transport performance. PES with 1 wt% TiO_2 was positioned in the lower-right quadrant of the diagram, indicating a "sieve-in-a-cage" morphology. In this case, while gas permeability increased, the non-ideal morphology led to a decrease in gas pair selectivity (CO_2/CH_4). In contrast, PES containing 3 wt% and 5 wt% TiO_2 were in the upper-right quadrant, reflecting ideal morphology. This suggests strong interfacial interactions between the polymer chains and the filler surface, which enhanced the overall performance of the MMMs. Notably, the 3 wt% TiO_2 loading demonstrated better performance in terms of relative selectivity compared to the 5 wt% loading. Although gas permeation was not significantly improved, the selectivity was superior, indicating optimal interfacial interactions at this filler concentration. Overall, the results highlight that a good interfacial interaction exists between PES and TiO_2 at filler loadings of 3 to 5 wt%, with 3 wt% offering the best balance between selectivity and interfacial compatibility.

4 Conclusion

This study investigates TiO_2 with PES to create MMMs with enhanced properties. The combination of PES and TiO_2 was chosen to leverage their complementary gas separation characteristics. The blend exhibited miscibility across all compositions, likely due to hydrogen bonding, as was confirmed by the characterizations. The resulting MMMs displayed a homogeneous morphology with finger-like pore formation. The thermal stability was between that of the individual polymers and increased with higher PES concentrations. Notably, the MMMs outperformed the individual polymer membranes in terms of permeability and selectivity. The addition of TiO_2 to PES membranes significantly boosted the separation performance, yielding a 21.9% increase in selectivity. These MMMs offer a promising approach to optimizing cost and performance in PES–TiO_2 membrane development.

Acknowledgements

The work is supported by the National Research Program for Universities (NRPU), Higher Education Commission Pakistan, No. 20-15709/NRPU/R&D/HEC/2021.

References

[1] Bragança, I., Sánchez-Soberón, F., Pantuzza, G. F., Alves, A., Ratola, N. "Impurities in biogas: Analytical strategies, occurrence, effects and removal technologies", Biomass and Bioenergy, 143, 105878, 2020. https://doi.org/10.1016/j.biombioe.2020.105878

[2] Elkhalifah, A. E. I., Maitra, S., Bustam, M. A., Murugesan, T. "Effects of exchanged ammonium cations on structure characteristics and CO_2 adsorption capacities of bentonite clay", Applied Clay Science, 83–84, pp. 391–398, 2013. https://doi.org/10.1016/j.clay.2013.07.016

[3] Farnam, M., bin Mukhtar, H., bin Mohd Shariff, A. "A Review on Glassy and Rubbery Polymeric Membranes for Natural Gas Purification", ChemBioEng Reviews, 8(2), pp. 90–109, 2021. https://doi.org/10.1002/cben.202100002

[4] Jamil, A., Ching, O. P., Shariff, A. B. M. "Current Status and Future Prospect of Polymer-Layered Silicate Mixed-Matrix Membranes for CO_2/CH_4 Separation", Chemical Engineering & Technology, 39(8), pp. 1393–1405, 2016. https://doi.org/10.1002/ceat.201500395

[5] Goh, P. S., Ismail, A. F., Sanip, S. M., Ng, B. C., Aziz, M. "Recent advances of inorganic fillers in mixed matrix membrane for gas separation", Separation and Purification Technology, 81(3), pp. 243–264, 2011. https://doi.org/10.1016/j.seppur.2011.07.042

[6] Olajire, A. A. "CO_2 capture and separation technologies for end-of-pipe applications – A review", Energy, 35(6), pp. 2610–2628, 2010. https://doi.org/10.1016/j.energy.2010.02.030

[7] Park, H. B., Kamcev, J., Robeson, L. M., Elimelech, M., Freeman, B. D. "Maximizing the right stuff: The trade-off between membrane permeability and selectivity", Science, 356(6343), eaab0530, 2017. https://doi.org/10.1126/science.aab0530

[8] Robeson, L. M. "The upper bound revisited", Journal of Membrane Science, 320(1–2), pp. 390–400, 2008. https://doi.org/10.1016/j.memsci.2008.04.030

[9] Baker, R. W., Low, B. T. "Gas Separation Membrane Materials: A Perspective", Macromolecules, 47(20), pp. 6999–7013, 2014. https://doi.org/10.1021/ma501488s

[10] Nasir, R., Mukhtar, H., Man, Z., Shaharun, M. S., Bakar, M. Z. A. "Development and Performance Prediction of Polyethersulfone-Carbon Molecular Sieve Mixed Matrix Membrane for CO_2/CH_4 Separation", Chemical Engineering Transactions, 45, pp. 1417–1422, 2015. https://doi.org/10.3303/CET1545237

[11] Liang, C.-Y., Uchytil, P., Petrychkovych, R., Lai, Y.-C., Friess, K., Sipek, M., Mohan Reddy, M., Suen, S.-Y. "A comparison on gas separation between PES (polyethersulfone)/MMT (Na-montmorillonite) and PES/TiO_2 mixed matrix membranes", Separation and Purification Technology, 92, pp. 57–63, 2012. https://doi.org/10.1016/j.seppur.2012.03.016

[12] Arthanareeswaran, G., Starov, V. M. "Effect of solvents on performance of polyethersulfone ultrafiltration membranes: Investigation of metal ion separations", Desalination, 267(1), pp. 57–63, 2011. https://doi.org/10.1016/j.desal.2010.09.006

[13] Mahajan, R., Burns, R., Schaeffer, M., Koros, W. J. "Challenges in forming successful mixed matrix membranes with rigid polymeric materials", Journal of Applied Polymer Science, 86(4), pp. 881–890, 2002. https://doi.org/10.1002/app.10998

[14] Lin, H., Yavari, M. "Upper bound of polymeric membranes for mixed-gas CO_2/CH_4 separations", Journal of Membrane Science, 475, pp. 101–109, 2015. https://doi.org/10.1016/j.memsci.2014.10.007

[15] Kalantari, K., Moradihamedani, P., Ibrahim, N. A., Abdullah, A. H. B., Afifi, A. B. M. "Polysulfone mixed-matrix membrane incorporating talc clay particles for gas separation", Polymer Bulletin, 75(8), pp. 3723–3738, 2018. https://doi.org/10.1007/s00289-017-2234-5

[16] Ahn, J., Chung, W.-J., Pinnau, I., Guiver, M. D. "Polysulfone/silica nanoparticle mixed-matrix membranes for gas separation", Journal of Membrane Science, 314(1–2), pp. 123–133, 2008. https://doi.org/10.1016/j.memsci.2008.01.031

[17] Henis, J. M. S., Tripodi, M. K. "Composite hollow fiber membranes for gas separation: the resistance model approach", Journal of Membrane Science, 8(3), pp. 233–246, 1981. https://doi.org/10.1016/S0376-7388(00)82312-1

[18] Henis, J. M. S., Tripodi, M. K. "The Developing Technology of Gas Separating Membranes", Science, 220(4592), pp. 11–17, 1983. https://doi.org/10.1126/science.220.4592.11

[19] Ismail, N. M., Jakariah, N. R., Bolong, N., Anissuzaman, S. M., Nordin, N. A. H. M., Razali, A. R. "Effect of Polymer Concentration on the Morphology and Mechanical Properties of Asymmetric Polysulfone (PSf) Membrane", Journal of Applied Membrane Science & Technology, 21(1), pp. 33–41, 2017. https://doi.org/10.11113/amst.v21i1.107

[20] Andrady, A. L., Merkel, T. C., Toy, L. G. "Effect of Particle Size on Gas Permeability of Filled Superglassy Polymers", Macromolecules, 37(11), pp. 4329–4331, 2004. https://doi.org/10.1021/ma049510u

[21] Matteucci, S., Kusuma, V. A., Sanders, D., Swinnea, S., Freeman, B. D. "Gas transport in TiO_2 nanoparticle-filled poly(1-trimethylsilyl-1-propyne)", Journal of Membrane Science, 307(2), pp. 196–217, 2008. https://doi.org/10.1016/j.memsci.2007.09.035

[22] Merkel, T. C., Freeman, B. D., Spontak, R. J., He, Z., Pinnau, I., Meakin, P., Hill, A. J. "Sorption, Transport, and Structural Evidence for Enhanced Free Volume in Poly(4-methyl-2-pentyne)/Fumed Silica Nanocomposite Membranes", Chemistry of Materials, 15(1), pp. 109–123, 2003. https://doi.org/10.1021/cm020672j

[23] Takahashi, S., Paul, D. R. "Gas permeation in poly(ether imide) nanocomposite membranes based on surface-treated silica. Part 1: Without chemical coupling to matrix", Polymer, 47(21), pp. 7519–7534, 2006. https://doi.org/10.1016/j.polymer.2006.08.029

[24] Matteucci, S., Kusuma, V. A., Kelman, S. D., Freeman, B. D. "Gas transport properties of MgO filled poly(1-trimethylsilyl-1-propyne) nanocomposites", Polymer, 49(6), pp. 1659–1675, 2008. https://doi.org/10.1016/j.polymer.2008.01.004

[25] Matteucci, S., Raharjo, R. D., Kusuma, V. A., Swinnea, S., Freeman, B. D. "Gas Permeability, Solubility, and Diffusion Coefficients in 1,2-Polybutadiene Containing Magnesium Oxide", Macromolecules, 41(6), pp. 2144–2156, 2008. https://doi.org/10.1021/ma702459k

[26] Adnan, M. A., Zainuddin, M. I. F., Ahmad, A. L. "The Effect of Concentration on PES/NMP System on Flat Sheet Membrane Fabrication and its Performance for CO_2 Gas Separation", Journal of Physical Science, 34(2), pp. 101–114, 2023. https://doi.org/10.21315/jps2023.34.2.8

[27] Moghadam, F., Omidkhah, M. R., Vasheghani-Farahani, E., Pedram, M. Z., Dorosti, F. "The effect of TiO_2 nanoparticles on gas transport properties of Matrimid5218-based mixed matrix membranes", Separation and Purification Technology, 77(1), pp. 128–136, 2011. https://doi.org/10.1016/j.seppur.2010.11.032

[28] Shi, F., Ma, Y., Ma, J., Wang, P., Sun, W. "Preparation and characterization of PVDF/TiO_2 hybrid membranes with different dosage of nano-TiO_2", Journal of Membrane Science, 389, pp. 522–531, 2012. https://doi.org/10.1016/j.memsci.2011.11.022

[29] Galaleldin, S., Mannan, H. A., Mukhtar, H. "Development and characterization of polyethersulfone/TiO_2 mixed matrix membranes for CO_2/CH_4 separation", AIP Conference Proceedings, 1901(1), 130017, 2017. https://doi.org/10.1063/1.5010577

[30] Asgarkhani, M. A. H., Mousavi, S. M., Saljoughi, E. "Cellulose acetate butyrate membrane containing TiO_2 nanoparticle: Preparation, characterization and permeation study", Korean Journal of Chemical Engineering, 30(9), pp. 1819–1824, 2013. https://doi.org/10.1007/s11814-013-0122-8

[31] Reza, A., Seyed, M. M., Reza, A. "Effect of sonochemical synthesized TiO_2 nanoparticles and coagulation bath temperature on morphology, thermal stability and pure water flux of asymmetric cellulose acetate membranes prepared via phase inversion method", Chemical Industry and Chemical Engineering Quarterly, 18(3), pp. 385–398, 2012. https://doi.org/10.2298/CICEQ111202014A

[32] Muruganandam, N., Paul, D. R. "Gas sorption and transport in miscible blends of tetramethyl bisphenol-A polycarbonate and polystyrene", Journal of Polymer Science Part B: Polymer Physics, 25(11), pp. 2315–2329, 1987. https://doi.org/10.1002/polb.1987.090251109

[33] Jamil, A., Zulfiqar, M., Arshad, U., Mahmood, S., Iqbal, T., Rafiq, S., Iqbal, M. Z. "Development and Performance Evaluation of Cellulose Acetate-Bentonite Mixed Matrix Membranes for CO_2 Separation", Advances in Polymer Technology, 2020(1), 8855577, 2020. https://doi.org/10.1155/2020/8855577

[34] Nyflött, Å., Petkova-Olsson, Y., Moons, E., Bonnerup, C., Järnström, L., Carlsson, G., Lestelius, M., Minelli, M. "Modeling of oxygen permeation through filled polymeric layers for barrier coatings", Journal of Applied Polymer Science, 134(20), 44834, 2017. https://doi.org/10.1002/app.44834

[35] Moradihamedani, P., Ibrahim, N. A., Yunus, W. M. Z. W., Yusof, N. A. "Study of morphology and gas separation properties of polysulfone/titanium dioxide mixed matrix membranes", Polymer Engineering and Science, 55(2), pp. 367–374, 2015. https://doi.org/10.1002/pen.23887

[36] Rashid, M. H., Farrukh, S., Javed, S., Hussain, A., Fan, X., Ali, S., Ayoub, M. "Synthesis and gas permeation analysis of TiO_2 nanotube-embedded cellulose acetate mixed matrix membranes", Chemical Papers, 74(3), pp. 821–828, 2020. https://doi.org/10.1007/s11696-019-00913-8

[37] Maqsood, K., Jamil, A., Ahmed, A., Sutisna, B., Nunes, S., Ulbricht, M. "Effect of TiO_2 on Thermal, Mechanical, and Gas Separation Performances of Polyetherimide–Polyvinyl Acetate Blend Membranes", Membranes, 13(8), 734, 2023. https://doi.org/10.3390/membranes13080734

[38] Moore, T. T., Koros, W. J. "Non-ideal effects in organic–inorganic materials for gas separation membranes", Journal of Molecular Structure, 739(1–3), pp. 87–98, 2005. https://doi.org/10.1016/j.molstruc.2004.05.043

[39] Hashemifard, S. A., Ismail, A. F., Matsuura, T. "Mixed matrix membrane incorporated with large pore size halloysite nanotubes (HNTs) as filler for gas separation: Morphological diagram", Chemical Engineering Journal, 172(1), pp. 581–590, 2011. https://doi.org/10.1016/j.cej.2011.06.031

[40] Jamil, A., Oh, P. C., Shariff, A. M. "Polyetherimide-montmorillonite mixed matrix hollow fibre membranes: Effect of inorganic/organic montmorillonite on CO_2/CH_4 separation", Separation and Purification Technology, 206, pp. 256–267, 2018. https://doi.org/10.1016/j.seppur.2018.05.054